

Damping Characteristics of Fibre Reinforced Polymers

H. Hanselka, U. Hoffmann

Besides the advantage of high stiffness and stability related to weight, dynamically loaded lightweight structures of modern fibre composites show outstanding damping properties. Undesirable vibration and resonance effects can largely be avoided by specific selection and lay-up of reinforcement and matrix material in the composite. For this purpose all dynamically relevant material characteristics need to be known for the dynamical design and optimisation of a structure. This paper shall give a contribution to the experimental determination and to the analytical processing of these characteristics. A great number of combinations of different materials, composite lay-ups and environmental parameters like temperature, frequency, humidity, etc. determine the anisotropic composite damping. Using the homogeneous, orthotropic viscoelastic behaviour of a single layer measured by means of the resonance frequency method a generalised classical lamination theory is applied to calculate the anisotropic damping of the composite laminate. Regarding the frequency and temperature influence on the dynamical behaviour of polymer materials, experience is required concerning the relevant material properties of fibre composites. Based on this knowledge new design criteria can be presented and a material selection specifically designed for dynamically loaded lightweight structures becomes possible.

1 Introduction

Fibre reinforced polymers are increasingly applied to components under high dynamic loads. A wide range of applications can be found in aircraft and vehicle design as well as in machine tool engineering, robotics and general mechanical engineering. Fibre composite technology allows the customer to select the material combinations, the fibre orientations, and the composite lay-up in order to improve the material damping. Economic reasons require new manufacturing technologies using fibre composites to produce large, single components. Joints between structural components are minimised. Since they usually determine a favourable vibration behaviour new damping concepts are required for the design of structures from fibre composites.

In this paper a practical procedure is given for the determination of the most important damping characteristics of an elementary single layer out of fibre composites in-axis as well as off-axis. The procedure is based on resonance frequency results extended to a combined bending, torsional and longitudinal oscillator. Furthermore analysis methods are described for the design of multilayer composites optimised with respect to damping and stiffness. The mathematical-mechanical modelling is based on the correspondence principle of the theory of linear viscoelasticity. The model is first applied to unidirectional composite as a basic element. Subsequently, stiffness and damping characteristics of multilayer fibre composites are determined and optimised using the concept of complex moduli. Structural optimisation bases on the knowledge of the material properties of the UD layer from which the anisotropic composite properties are derived. Parameters like temperature and humidity affect the material properties and must also be considered.

2 Experimental Procedure for Determination of Damping Characteristics

In technical constructions the fading of vibrations is named damping. Here, the mechanical (kinetic) energy contained in the system is transformed into heat. These dissipation processes inside the materials are called material damping.

Material damping is introduced into the conditions of elastic deformation on the basis of harmonic stresses and deformations. Assuming harmonic stresses $\sigma^*(t, \omega) = \sigma^*(\omega) \cdot e^{j\omega t}$ and corresponding strains $\varepsilon^*(t, \omega) = \varepsilon^*(\omega) \cdot e^{j\omega t}$ and with the assumption of the theory of linear viscoelasticity the following one-dimensional material law can be defined:

$$\sigma^*(\omega) = E^*(\omega) \cdot \varepsilon^*(\omega) = (E'(\omega) + i \cdot E''(\omega)) \cdot \varepsilon^*(\omega) = E'(\omega) \cdot (1 + i \cdot d(\omega)) \cdot \varepsilon^*(\omega) \quad (1)$$

with $d(\omega)$ as material damping and $E'(\omega)$ as the dynamical Young's modulus or energy storage modulus. ($E''(\omega)$ is called loss modulus).

This is one way to describe linear viscoelastic material behaviour, other methods like e.g. the energy method are also possible.

For common fibre volume contents of 50 to 60% and with a comparably low strain level in the structure, linear damping mechanisms predominate in most cases (Ehrenstein, 1998; Tauchert, 1974). Thus, in the following linear damping $d(\omega)$ will be considered exclusively where the reinforcing fibre shows linear elastic behaviour and the polymer matrix is linearly viscoelastic (Tauchert, 1974; Achenbach, 1975; Niederstadt and Hanselka, 1989). If synthetic fibres, e.g. aramide, are used as reinforcing material, the fibres also show damping. Corresponding approaches are available in the literature (Hanselka, 1992).

In order to determine the damping characteristics of polymer fibre composites a specific resonance method with small strain amplitudes ($\epsilon < 0,001$) was developed for the above mentioned linear relations. With this resonance method damping and corresponding dynamical properties of samples with rectangular cross-sections can be simultaneously determined for bending and torsional vibrations. In the experimental set up a cantilever bar is excited to bending and torsional vibrations at adjustable temperature (Figure 1). The excitation is realised by an eccentric force $F(t)$ generated by an inductive shaker. Next to the clamping the vibration $\omega_0(t)$ is measured by means of an eddy current sensor.

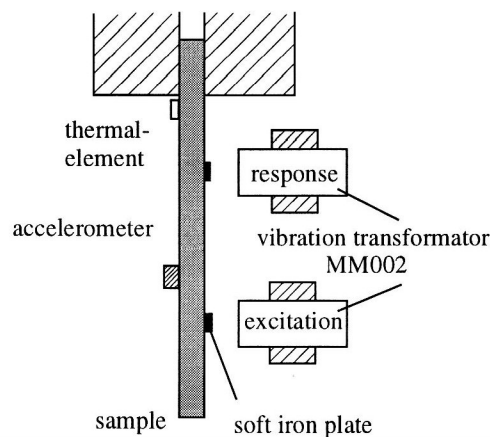


Figure 1. Resonance Bending and Torsional Vibration Experiment, Schematic

Longitudinal vibrations can be applied in a corresponding set up. Here the sample bar is freely suspended by filaments and two identical masses are fixed to its ends to lower the natural frequencies. Longitudinal vibrations are broadband excited by means of an electromagnetic shaker and the response is measured by an accelerometer. In both cases the signal processing is performed with a suitable amplifier technology and a Fourier analyser.

In case of a cantilever bar out of unidirectional glass-fibre reinforced plastic (GFRP-UD) four resonance peaks can be seen in the diagram (Figure 2). They represent the first three bending natural frequencies $f_{n,b}$ as well as the first torsional natural frequency $f_{1,t}$ (3rd peak) which appears strongly damped.

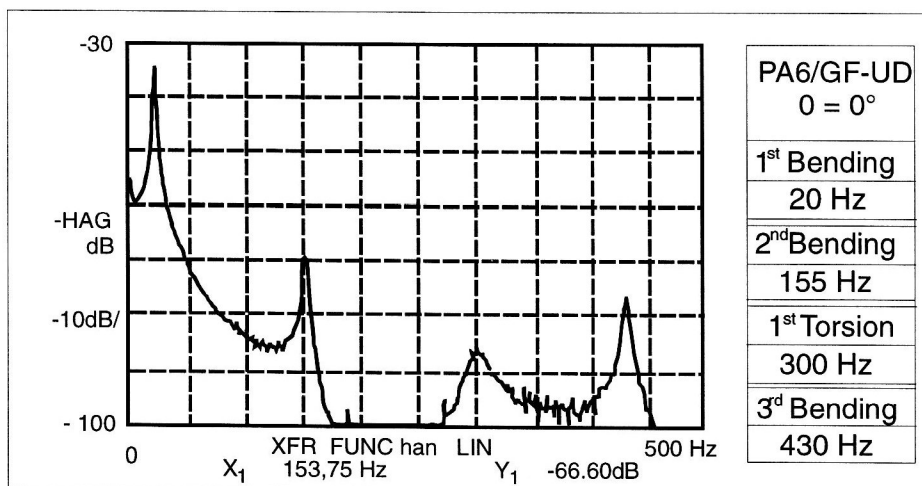


Figure 2. Resonance Diagram of a GFRP-UD Bar in Case of Bending and Torsional Vibrations

Evaluation of the material characteristics from the resonance diagram is based on the equations of motion for weakly dampened bending $w(x,t)$, torsional $\vartheta(x,t)$, and longitudinal $u(x,t)$ vibrations (Hanselka; 1992; Hoffmann, 1992). For a cantilever bar of rectangular cross-section with the dimensions $b \times h$ they read

$$E'(1 + id_B)I_y \frac{\partial^4 w(x,t)}{\partial x^4} + \rho b h \frac{\partial^2 w(x,t)}{\partial t^2} = 0 \quad (2)$$

$$G'(1 + id_T)I_t \frac{\partial^2 \vartheta(x,t)}{\partial x^2} + r b h \frac{b^2 + h^2}{12} \frac{\partial^2 \vartheta(x,t)}{\partial t^2} = 0 \quad (3)$$

$$E'(1 + id_L) \frac{\partial^2 u(x,t)}{\partial x^2} + \rho \frac{\partial^2 u(x,t)}{\partial t^2} = 0 \quad (4)$$

Separation of the variables leads to ordinary differential equations and by imposing the respective boundary conditions the resulting eigenvalue problems specify the resonance frequencies f_n .

The analytical resonance functions $w(x,f)$, $\vartheta(x,f)$, and $u(x,f)$ can be directly obtained from the experimentally determined transfer functions using the condition $f = f_n$, the dynamical Young's modulus E' , and the dynamical shear modulus G' . The corresponding degrees of damping d_B (bending damping), d_T (torsional damping), and d_L (longitudinal damping) are given by the half bandwidth Δf of the resonance peak over f_n , taken at a decrease of 3 dB on both sides of the peak. The resonance method can be applied for damping factors up to $d = 10\%$. For a precise evaluation the resonance curve is zoomed at the resonance frequency f_n . In addition the curve can be analysed by means of a computer-aided curve fitting, using a discrete model with selectable degrees of freedom (Hufenbach and Hoffmann, 1991).

3 Results of Experimental Investigations

3.1 Temperature Influence on the Damping Characteristics

Polymere materials show material properties which strongly depend on temperature and frequency. In glass state they have a high storage modulus but low damping. With increasing temperature the degree of damping shows several maxima, each of which is combined with a change in the modulus. In the range of softening, a substantial decrease of the storage modulus appears whereas the damping shows a maximum. The frequency gains considerable influence on the damping and stiffness behaviour. In this case, highest molecule mobility occurs at the temperature of maximum damping (Figure 3).

The beginning of the steep decline of the storage modulus generally represents the limit of technical application of (fibre reinforced) polymers; it is named glass transition point. The position of the glass transition point depends on the frequency and on the absorbed humidity. Water absorption in polymere materials results in a change in viscoelastic behaviour. In the case of constant frequency a higher humidity reduces the glass transition point to lower temperatures and at constant temperature transition occurs at shorter cycle times or at higher frequencies, respectively.

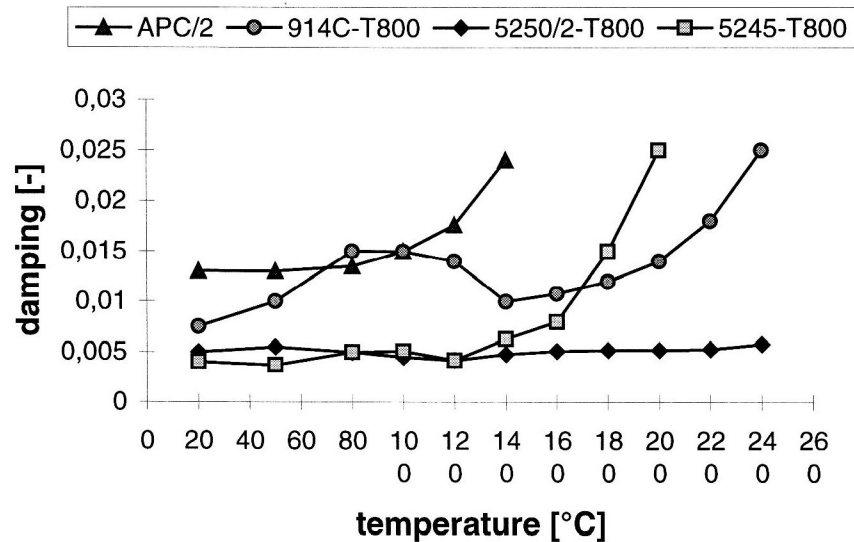


Figure 3. Temperature Dependent Damping Characteristics of Different Bidirectionally Reinforced Carbon Fibre Composites

Several matrices, bidirectionally ($\theta = \pm 45^\circ$) reinforced with the carbon fibres (T800 and T300, respectively), have been analysed in the resonance bending vibration test to investigate the temperature influence on the damping characteristics. Detailed results for a temperature range between 20°C and 240°C are given in (Hanselka, 1992). The bismaleinimid matrix RIGIDITE 5250 shows relatively small damping which is constant across the entire range of temperature. Polyetheretherketon (APC/2) with a glass transition temperature near 140°C has a much higher damping. At room temperature the matrix RIDIGITE 5245, consisting of epoxy and bismaleinimid, has just as little damping as RIGIDITE 5250. A secondary dispersion appears at $T=100^\circ\text{C}$. There the dissipated energy is 25% higher as compared to room temperature. With further temperature increase the damping decreases again until a minimum at $T = 140^\circ\text{C}$. Above $T = 140^\circ\text{C}$ the damping increase continuously until the glass transition point of the main component of the matrix is reached. For FIBREDUX 914C the secondary dispersion is even more dominant. Starting from room temperature the energy dissipation increases and reaches its first maximum at $T=80^\circ\text{C}$. Here, the damping is twice as high as at room temperature. Above $T=120^\circ\text{C}$ damping decreases drastically until near $T=200^\circ\text{C}$ a steep rise up to the glass transition point starts. Such a behaviour is due to the fact that the resin system 914C consists of a great number of components with different glass transition points.

Composites with glass transition temperatures of 180°C and higher can be set up by mixing matrices which show outstanding damping properties already at low and medium temperatures and no significant loss in stiffness. This can be demonstrated with the material VICOTEX 6376 / HTA7.

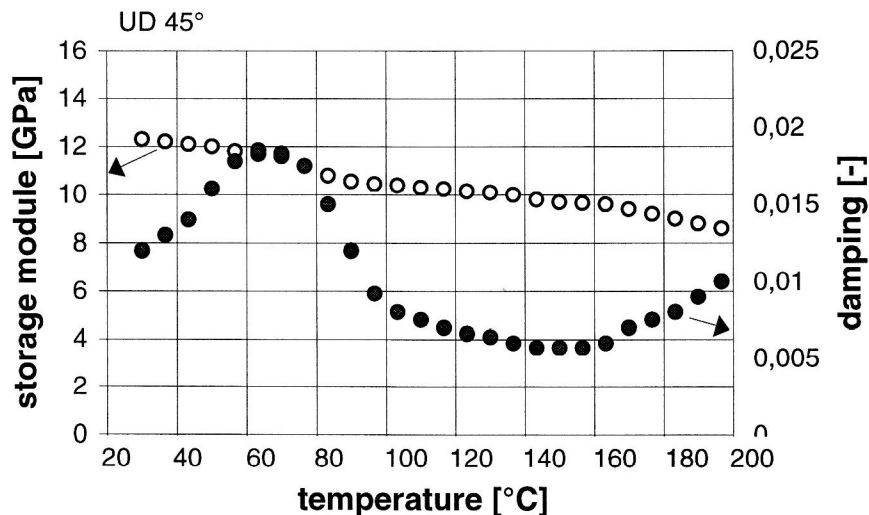


Figure 4. Temperature Dependent Stiffness and Damping Characteristics of the UD Material 6376/HTA7 with 45° Fibre Orientation

The primary damping maximum occurs at a temperature of $T=60^\circ\text{C}$, independent of the fibre orientation but with different significance (Figure 4). This secondary dispersion field is less pronounced than the one at the glass transition point expected at $T=220^\circ\text{C}$. However, a considerable increase of the damping with only small stiffness loss compared to room temperature is reachable. The relation of maximum damping at $T=60^\circ\text{C}$ to the one at room temperature is very high. Thus, depending on the laminate lay-up, an increase of damping up to 333% can be achieved by an insignificant increase of temperature.

3.2 Influence of Humidity

Humidity is an environmental parameter which has to be considered for the analysis of (dynamically) loaded fibre composite structures. Polymere matrices and synthetic fibres absorb moisture from the environment. The amount of absorbed water depends on time, surrounding humidity and the diffusion coefficient of the material. Regarding glass and carbon fibre reinforced polymers humidity leads to a degradation of the matrix dependent strength and stiffness properties. If synthetic fibres are used as reinforcing material also the fibre dependent properties are affected. On the other hand a higher humidity increases the maximum allowable strain of the polymere material.

The humidity influence on the damping behaviour of fibre composites is determined by means of the resonance bending test. Unidirectionally fibre reinforced samples (material: 6376-T400), conditioned with 0% and 75% relative humidity, were tested at fibre angles of $\theta=0^\circ$, $\theta=45^\circ$ and $\theta=90^\circ$. The direction depending damping and stiffness behaviour of the dry and humid layer is compared in a polar diagram (Figure 5) (Hanselka, 1991). It shows the variation of the damping factor d_1 and the memory modulus E^*_1 with varying fibre angle θ where the

functions between the measured values are obtained by a transformation analysis. Only one quarter of the double symmetric polar diagram is significant. For all reinforcing directions a relative humidity of 75% increases the damping by a factor of two whereas stiffness is reduced by approx. 20%. In humid laminates the damping maximum shifts to $\theta=39^\circ$ from $\theta=45^\circ$ for the dry ones. It can be concluded that the damping characteristics of dynamically loaded fibre composite structures are improved considerably by the influence of humidity. Therefore, using damping characteristics obtained under dry conditions leads to conservative results. The shift of the damping maximum towards smaller fibre angles even increases the potential of optimisation.

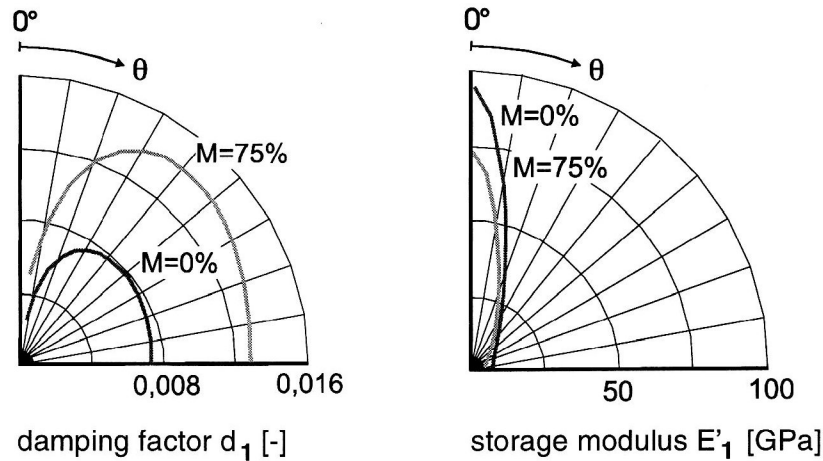


Figure 5. Damping and Stiffness of a Unidirectionally Carbon Fibre Reinforced Polymer (6376-T400) for Various Fibre Angles and Different Humidity

With an additional thermal load these effects appear even stronger. Material damping increases considerably whereas stiffness is reduced. The thermal resistance of the composite structure decreases up to 50% compared to the dry state depending on the matrix material and humidity.

4 Determination of Material Damping for Multi-Layer Fibre Composites

Glass fibre reinforced (GF) plastics with a matrix of epoxy resin (EP) and carbon fibre reinforced (CF) plastics with matrices of epoxy resin and Bismaleinimid (BMI) were selected from the great number of fibre matrix combinations available for lightweight construction. With these materials multi-layer composite structures can be set up using uni-directionally (UD) reinforced prepregs. In Table 1 the static and dynamic characteristics of the investigated UD laminates are summarised.

Material	EP/GF-UD		EP/CF-UD		BMI/CF-UD	
Components	E-glass	EPLY556 HT 976	T400	EP 6376	T 800	BMI 5245
Young's modulus [GPa]	73	3,5	250	3,3	294	3,3
Poisson number ν	0,18	0,35	0,24	0,36	0,23	0,33
Density ρ [kg/m ³]	2520	1220	1800	1230	1810	1250
Strain to failure ϵ_{Br} [%]	2,5	4	1,5	4	3,2	4
Composite	UD (10:1)		UD		UD	
Fibre vol. fraction ϕ [%]	56+1,0		56+1,0		62+1,0	
Young's moduli	static	dynamic	static	dynamic	static	dynamic
E_1 [GPa] (axial)	41	33,5	137,16	94,79	175	94
E_2 [GPa] (transversal)	15	14	9,14	7,8	12	6,4
ν_{12}		0,24		0,2914		0,32
G_{12} [GPa]	3,6	4,7	19	5,28	6	4,6
Damping						
d_1 (axial) [%]		0,1875		0,1726		0,0835
d_2 (transversal) [%]		0,6988		0,7158		0,3249
d_{12} (shear) [%]		1,1662		0,8204		0,3510

Table 1. Characteristics of the Investigated Materials

For simplicity reasons the single layer is described as a uniform continuum with anisotropic, linear viscoelastic properties.

To introduce the damping to fibre composites the concept of the complex moduli (Hashin, 1970; Schultz and Tsai, 1975) is applied to the constitutive (material) equations by replacing the elementary elastic constants by their corresponding viscoelastic ones. Referring to a fibre fixed 1,2,3 coordinate system the orthotropic viscoelastic material law reads

$$\begin{aligned}\varepsilon_1^* &= S_{11}^* \cdot \sigma_1^* + S_{12}^* \cdot \sigma_2^* \equiv \frac{1}{E_1^*} \cdot \sigma_1^* - \frac{\nu_{12}}{E_1^*} \cdot \sigma_2^* \\ \varepsilon_2^* &= S_{12}^* \cdot \sigma_1^* + S_{22}^* \cdot \sigma_2^* \equiv -\frac{\nu_{12}}{E_1^*} \cdot \sigma_1^* + \frac{1}{E_2^*} \cdot \sigma_2^* \\ \gamma_{12}^* &= S_{66}^* \cdot \tau_{12}^* \equiv \frac{1}{G^*} \cdot \tau_{12}^*\end{aligned}\quad (5)$$

Consequently, a damping is assigned to every dynamic Young's modulus:

$$\begin{aligned}E_1^* &= E_1' \cdot (1 + d_1) & G_{12}^* &= G_{12}' \cdot (1 + d_{12}) \\ E_2^* &= E_2' \cdot (1 + d_2) & \nu_{12}^* &= \nu_{12}' = \nu_{12}\end{aligned}\quad (6)$$

In the following, d_1 is designated as axial damping, d_2 as transversal damping, and d_{12} as shear damping. For each single layer of the multiple layer composite six dynamic characteristics have to be determined experimentally.

Assuming that the damping is small ($d^2 \ll 1$), which is suitable for polymere fibre composites, the stiffness and compliance of a single orthotropic layer can be specified as

$$\begin{aligned}Q_{ij}^* &= Q_{ij}' + i \cdot Q_{ij}'' = Q_{ij}' (1 + i \cdot d_{Q_{ij}}) \\ \text{and} \quad S_{ij}^* &= S_{ij}' + i \cdot S_{ij}'' = S_{ij}' (1 + i \cdot d_{S_{ij}})\end{aligned}\quad (7)$$

Stiffness		Compliance	
Modulus	Damping	Modulus	Damping
$Q_{11}' = \frac{E_1'}{1 - \nu_{12}^2 \frac{E_2'}{E_1'}}$	$d_{Q_{11}} = d_1 + (d_2 - d_1) \frac{E_2' \cdot \nu_{12}^2}{E_1' - E_2' \cdot \nu_{12}^2}$	$S_{11}' = \frac{1}{E_1'}$	$d_{S_{11}} = -d_1$
$Q_{12}' = \frac{\nu_{12} E_2'}{1 - \nu_{12}^2 \frac{E_2'}{E_1'}}$	$d_{Q_{12}} = d_2 + (d_2 - d_1) \frac{E_2' \cdot \nu_{12}^2}{E_1' - E_2' \cdot \nu_{12}^2}$	$S_{12}' = -\frac{\nu_{12}}{E_2'}$	$d_{S_{12}} = -d_2$
$Q_{22}' = \frac{E_2'}{1 - \nu_{12}^2 \frac{E_2'}{E_1'}}$	$d_{Q_{22}} = d_2 + (d_2 - d_1) \frac{E_2' \cdot \nu_{12}^2}{E_1' - E_2' \cdot \nu_{12}^2}$	$S_{22}' = \frac{1}{E_2'}$	$d_{S_{22}} = -d_2$
$Q_{66}' = G_{12}'$	$d_{Q_{66}} = d_{12}$	$S_{66}' = \frac{1}{G_{12}'}$	$d_{S_{66}} = -d_{12}$

In the following a multilayer fibre composite is considered with a constant thickness h ($h \ll$ length a , width b) consisting of N single orthotropic layers (index k , thickness h_k). Each single layer may be oriented at a certain angle with respect to the global x,y -system of the multi-layer composite. In order to set up a material law for the multi-layer composite the reduced layer stiffness values Q_{ij}^* as given in equation (7) must be transformed leading to the coefficients \tilde{Q}_{ij}^* of the global coordinate system

For further considerations it can be referred to the fundamental assumptions of the classical laminate theory, e.g., (Whitney and Rosen, 1987). With the introduction of the complex membrane forces per unit length n_i^* and the corresponding moments m_i^* as well as the strains ε_j^{0*} and curvature κ_j^* of the centre plane, the following complex constitutive equations of the multilayer composite can be derived (in pseudo-vector spelling):

$$\begin{pmatrix} n_i^* \\ m_i^* \end{pmatrix} = \begin{bmatrix} A_{ij}^* & B_{ij}^* \\ B_{ij}^* & D_{ij}^* \end{bmatrix} \cdot \begin{pmatrix} \varepsilon_j^{0*} \\ \kappa_j^* \end{pmatrix} \quad (i, j = 1, 2, 6)\quad (9)$$

with the components of the symmetric submatrices

$$\begin{aligned} A_{ij}^* &= \sum_{k=1}^N \bar{Q}_{ij}^{*(k)} h_k & B_{ij}^* &= \sum_{k=1}^N \bar{Q}_{ij}^{*(k)} z_k h_k & D_{ij}^* &= \sum_{k=1}^N \bar{Q}_{ij}^{*(k)} \left(z_k^2 h_k + \frac{h_k^3}{12} \right) \end{aligned} \quad (10)$$

Membrane stiffness Coupling stiffness Plate stiffness

Using the modified plate stiffness

$$\bar{D}_{ij}^* = D_{ij}^* - B_{im}^* A_{mn}^{*-1} B_{nj}^* \quad (i, j, m, n = 1, 2, 6) \quad (11)$$

and neglecting membrane forces the complex moments are

$$m_i^* = \bar{D}_{ij}^* \kappa_j^* = \frac{h^3}{12} Q_{ij}^{*(MSV)} \kappa_j^* = \frac{h^3}{12} \left(Q_{ij}^{*(MSV)} + i Q_{ij}''^{(MSV)} \right) \quad (12)$$

For further consideration an additional multi-layer composite characteristic can be introduced derived from $Q_{ij}^{*(MSV)}$ as anisotropic bending stiffness. The inversion of $Q_{ij}^{*(MSV)}$ in accordance with

$$S_{ij}'^{(MSV)} = \left(Q_{ij}'^{MSV} + Q_{im}''^{(MSV)} \cdot Q_{mm}^{(MSV)-1} \cdot Q_{nj}''^{(MSV)} \right)^{-1} \quad \text{Storage part} \quad (13)$$

$$S_{ij}''^{(MSV)} = \left(-Q_{ij}''^{MSV} - Q_{im}'^{(MSV)} \cdot Q_{mm}^{(MSV)-1} \cdot Q_{nj}'^{(MSV)} \right)^{-1} \quad \text{Loss part}$$

results in the equation

$$\kappa_i^* = \frac{12}{h^3} \left(S_{ij}'^{(MSV)} + i S_{ij}''^{(MSV)} \right) \cdot m_j^* \quad (14)$$

A comparison with the elementary but complex differential equation of the bending curvature of an isotropic viscoelastic bar leads to the following equivalent dynamic characteristics for pure bending of the anisotropic multilayer composite (around an arbitrary axis):

$$E^{(MSV)} = \frac{1}{S_{11}'^{(MSV)}} \quad d^{(MSV)} = -\frac{S_{11}''^{(MSV)}}{S_{11}'^{(MSV)}} \quad (15)$$

Consequently, the following steps are necessary for the definition of damping characteristics of multilayer composites:

1. Measurement or analytical estimation (Hanselka, 1992) of the degree of damping d_1 , d_2 , d_{12} and the (dynamic) Young's moduli E'_1 , E'_2 , G'_{12} as well as ν_{12} for every single layer,
2. Calculation of the complex modified plate stiffness \bar{D}_{ij}^* considering the coupling properties,
3. Determination of the multi-layer composite compliances from the inversion of the modified plate stiffness,
4. Specification of equivalent damping $d^{(MSV)}$ and/or elasticity $E^{(MSV)}$ for a corresponding bending oscillator.

5 Experimental/Numerical Results of Material Damping for Different Laminates

5.1 Carbon Fibres as Reinforcing Material

Compared to other materials carbon fibres show small damping properties but very high stiffness. In order to identify the influence of different fibre types (T300, T800, and M46) on the damping and stiffness behaviour and their directional dependency they are measured for a single unidirectionally reinforced layer using the same matrix (LY556/HT976). A high fibre volume content of $\varphi=70\%$ was chosen so that the small differences in fibre damping are not fully covered by the viscoelastic behaviour of the matrix. The calculated dynamic laminate properties are shown in the polar diagrams of Figure 6.

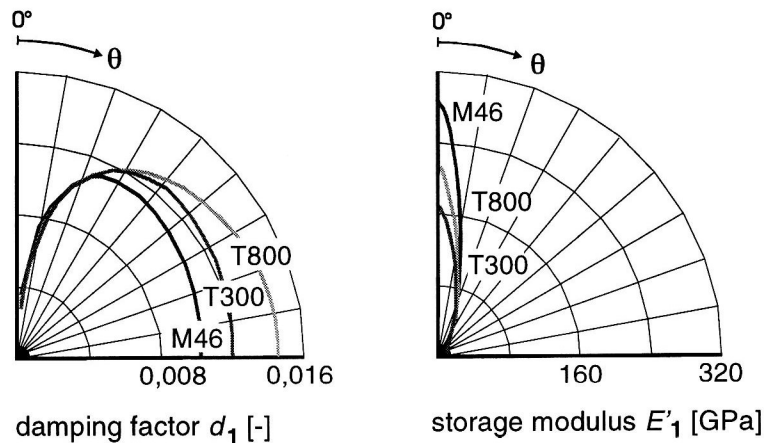


Figure 6. Directional Damping and Stiffness Behaviour of Different Carbon Fibres Embedded in the Matrix LY556/HT976, Fibre Volume Content $\varphi=70\%$

In fibre direction only small deviations in damping are recognisable, whereas great differences occur with increasing fibre angles. The highest energy absorption can be achieved with the high-tensile carbon fibre T800. The damping is 13% larger than those of the laminate with the fibre T300 and 22% larger as compared to the unidirectional composite with the high-modulus carbon fibre M46. The increase in damping with increasing fibre angle is equal for both high-tensile fibre types up to an angle of $\theta=30^\circ$ while for the high-modulus fibre the gradient is higher. Maximum damping for the fibre T800 is reached at a fibre orientation of $\theta=90^\circ$, for the fibre T300 at $\theta=45^\circ$ and for M46 at $\theta=34^\circ$.

Variation of the stiffness with fibre angle makes obvious the significant anisotropy of the laminates. The laminate with the high-modulus fibre M46 shows almost double the storage modulus in fibre direction as compared to that with the fibre T300. Nevertheless, the influence of the different reinforcing fibres can be neglected already at a fibre angle of $\theta=20^\circ$. The laminate with the high-modulus fibre even shows the lowest storage modulus at $\theta=90^\circ$. It becomes clear that the dynamic behaviour of the carbon fibre reinforced laminates with low viscoelastic properties can be significantly influenced by the fibre angle.

5.2 Influence of Other Reinforcing Fibres

Much higher damping can be achieved with other fibre materials but at the expense of stiffness. In particular synthetic fibre reinforced polymers are characterised by a remarkably high energy absorption. Figure 7 shows the dynamic properties storage moduli and damping for the reinforcing materials Aramid fibre and Dyneema fibre embedded in the matrix system LY556/HY917 with low damping.

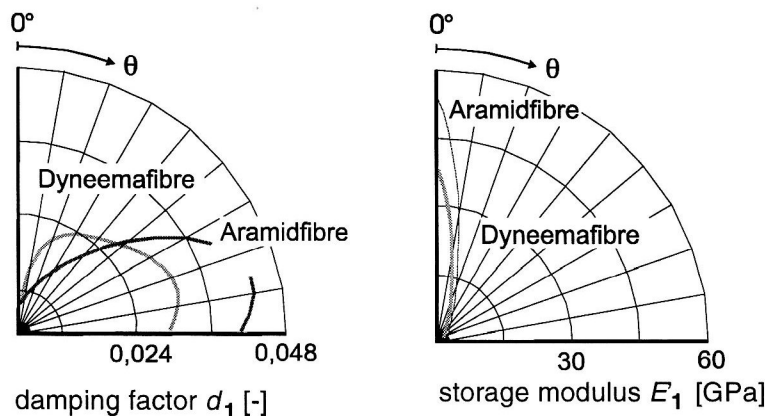


Figure 7. Direction depending damping and stiffness behaviour of different reinforcing fibres embedded in the same matrix LY556/HY917, fibre volume content $\varphi=60\%$

In fibre direction, the Aramid fibre reinforced laminate shows double the energy absorption as compared to the laminate with Dyneema fibre. Perpendicular to the fibre direction the difference is less distinct. The latter composite shows a sharp increase of damping with increasing fibre angle. Compared to the Aramid fibre reinforced

laminates a higher damping can be achieved with fibre angles $\theta=5^\circ$ and $\theta=40^\circ$. Considering also its extreme low density ($\rho=970 \text{ kg/m}^3$) makes Dyneema a very valuable damping material for lightweight structures. Damping of carbon fibre reinforced laminates (see Figure 6) is very small as compared to Aramid and Dyneema composites. However, with regard to the stiffness carbon fibres are superior.

5.3 Influence of the Matrix Material on the Viscoelasticity

The matrix system has a minor effect on the elastic properties of fibre composites, whereas its influence on damping is quite high. To illustrate this, matrices with different damping properties (LY556/HT976, 6376 and 5245) were uni-directionally reinforced with the identical fibres (T300) and their damping and stiffness behaviour was examined. The characteristics calculated for a fibre volume content $\varphi=50\%$ are plotted in Figure 8. With almost the same stiffness the different matrix materials show considerable differences in damping.

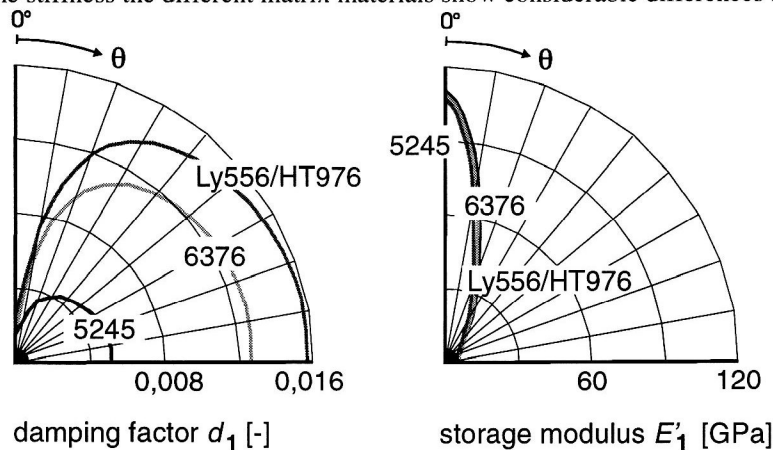


Figure 8. Directional Damping and Stiffness Behaviour of Different Matrices Uni-Directionally Reinforced with Carbon Fibre T300, Fibre Volume Content $\varphi=50\%$

For all laminates the maximum damping is at a fibre angle of $\theta=90^\circ$. The epoxy resin LY556/HT976 shows a three time higher damping compared to the modified Bismaleinimid 5245. The mixed matrix material 6376 has a 20% lower laminate damping.

5.4 Optimisation of Laminate Lay-Up

For UD-layers of the materials specified in Table 1 the polar diagrams of Figure 9 clearly show the counter rotation of the stiffness and damping characteristics. At a fibre angle of $\theta=0^\circ$ (load "on axis") the Young's modulus is always maximal (Figure 9, right) whereas the damping is a minimum (Figure 9, left). For the considered case of bending vibration the carbon fibre laminate with BMI matrix shows the highest stiffness, whereas the damping capabilities are comparably small. On the other hand, the glass fibre laminate with epoxy matrix has high damping properties but a small stiffness. The highest damping can be achieved with the matrix system EP 6376, reinforced with the carbon fibre T400.

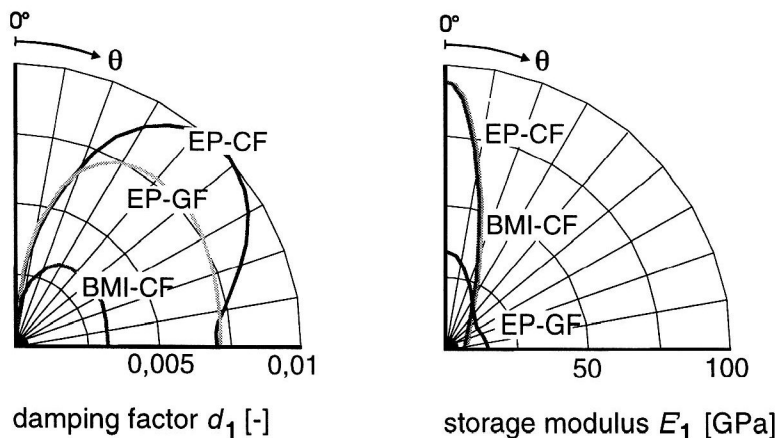


Figure 9. Comparison of the Dynamic Properties for Different Laminates

All considered laminates show a different but qualitatively similar fibre direction depending damping characteristics. Thus, the damping in all examined cases is not at its maximum at fibre orientation $\theta=90^\circ$, but with orientation between $15^\circ \leq \theta \leq 45^\circ$. Therewith, damping shows a similar direction depending behaviour as it is known for the Poisson's ratio of the UD layer. This can be physically explained by a dominant influence of the shear part due to τ_{12^*} on the entire damping potential.

For laminates the total thickness h has to be taken as a further optimisation parameter under the aspect of light-weight design, not allowing an arbitrary wall thickness for the benefit of an improved damping. Angle lay-ups with fibre orientations ($\theta/-\theta\dots$) from prepregs of equal thickness $h_k = 0,125$ mm have proved to be especially suitable for the optimisation of the laminate damping $d^{(MSV)}$ (Hoffmann, 1992). A plate stiffness D'_{11} of at least 500 Nm will be taken as a constraint. The layer orientations θ_k and the laminate thickness h serve as optimisation parameters. The optimisation procedure is shown in Table 2. A laminate with $\theta=\pm 18^\circ$ and a relative increase in thickness of 6,25% results in a damping increase of about 130% compared to a unidirectional composite. Applying this to a (normalised) cantilever bar the decay time of a [18/-18] laminate is reduced to 30 seconds as compared to 75 seconds for an equally normalised UD laminate. It is worth mentioning that this angle ply laminate shows not only a high damping of the bending vibrations of approximated 0,2% but also quite a high damping of the torsional vibration.

Fibre direction θ_k ($^\circ$)	Layer number N	Laminate thickness h (mm)	Plate stiffness D'_{11} (Nm)	Bending modulus $E^{(MSV)}$ (GPa)	Damping of multilayer composite $d^{(MSV)}$ (%)
[0]	32	4	504,568	93,965	0,0835
[13/-13...]	33	4,125	504,561	81,012	0,1383
[18/-18/...]s	34	4,25	506,702	68,664	0,1947
[25/-25]9s	36	4,5	508,882	48,211	0,2898
[34/-34]10s	40	5	517,414	27,013	0,3799

Table 2. Optimisation of a CFRP Multilayer Composite

6 Conclusion

New manufacturing technologies with fibre composites allow to minimise the assembling of different parts. Therefore, material damping must be optimised to maintain a desired decay behaviour of the structure. The material damping of fibre composites itself is dependent on different parameters. In this paper suitable damping characteristics and notes for the adjustment of a desired damping are given.

As expected the calculated and experimentally proved damping behaviour of UD laminates are minimal in fibre direction and generally behave in counter-rotation to the stiffness behaviour. Nevertheless, the significant damping maximum does not appear perpendicular to the fibre direction but rather at an intermediate orientation of $15^\circ \leq \theta \leq 45^\circ$, so that the corresponding points with sufficient stiffness have to be searched for in this range. For instance, the damping can be increase by 130% for a specific CFRP angle ply laminate with an insignificant increase in thickness of 6,25% only and with the same stiffness as compared to the UD laminate.

In future damping models must be introduced into numeric procedures such as the method of the finite elements (Schrader, 1997). However, since the optimum design of composite laminates requires a considerable effort alternative design tools such as the computer program LAMTECH (Herrmann et. al., 1992) should be considered.

Acknowledgement:

The authors wish to thank Dr.-Ing. habil. Klaus Rohwer, senior scientist at the Institute of Structural Mechanics of the German Aerospace Center (DLR), for the helpful discussions while reviewing this paper.

Literature

1. Achenbach, J.D.: A Theory of Elasticity with Microstructure for Directionally Reinforced Composites, Springer, New York, (1975).
2. Ehrenstein, G.W.: Dämpfungseigenschaften glasfaserverstärkter Kunststoffe, Kunststoffe 58, (1968), 12.

3. Hanselka, H.: Damping Behaviour of Unidirectional Fibre Reinforced Polymers, Nordwijk: ESA-SP-321, (1991).
 4. Hanselka, H.: Ein Beitrag zur Charakterisierung des Dämpfungsverhaltens polymerer Faserverbundwerkstoffe, Diss. Clausthal-Zellerfeld, (1992).
 5. Hashin, Z.: Complex Moduli of Viscoelastic Composites – II. Fiber Reinforced Materials, Int. Journal Solids Structures, Vol 6, (1970) .
 6. Herrmann, A.S.; Hanselka, H.; Haben, W.: Faserverbundwerkstoffe am Rechner komponieren, Kunststoffe 82, München, 1992.
 7. Hoffmann, U.: Zur Optimierung der Werkstoffdämpfung anisotroper polymerer Hochleistungs-Faserverbundstrukturen, Diss. Clausthal-Zellerfeld, (1992).
 8. Hufenbach, W.; Hoffmann, U.: Beitrag zur Optimierung der Steifigkeits- und Dämpfungskennwerte von Faserverbundstrukturen für dynamisch hochbeanspruchte Konstruktionen, Werkstoffe & Konstruktionen, 5, No. 2, (1991).
-
9. Niederstadt, G.; Hanselka, H.: Viskoelastizität und Dämpfung von CFK Prepreg-Verbunden, 28. Internationale Chemiefasertagung Dornbirn, (1989).
 10. Schrader, E.: Optimierung der Werkstoffdämpfung polymerer Faserverbundstrukturen mittels der Methode der Finiten Elemente, Shaker, Aachen 1998, Diss. RWTH Aachen, (1997).
 11. Schultz, A.B.; Tsai, S.W.: Measurement of Complex Dynamic Moduli for Laminated Fiber-Reinforced Composites, Springer, New York, (1975).
 12. Tauchert, T.R.: Internal Damping in a Fiber-Reinforced Composite Material, Journal of Composite Materials, 8, (1974).
 13. Whitney, J.M.; Rosen, B.W.: Structural Analysis of Laminated Anisotropic Plates, Technomic Publishing, Dayton, (1987).

Adresses: Prof. Dr.-Ing. Holger Hanselka, Otto-von-Guericke-Universität Magdeburg, Institut für Mechanik, Lehrstuhl für Adaptronik, Universitätsplatz 2, D-39106 Magdeburg, Dr.-Ing. Uwe Hoffmann, Kätnersredder Str. 135, D-24232 Schönkirchen